

การตรวจสอบการส่งผ่านคลื่นของหุ่นลอยกันคลื่น

ชัยยุทธ ชินณะราศรี¹ และ คมสัน วิริยกิจจา²

มหาวิทยาลัยเทคโนโลยีพระจอมเกล้าธนบุรี บางมด ทุ่งครุ กรุงเทพฯ 10140

บทคัดย่อ

ในงานวิจัยนี้ได้ทำการตรวจสอบการลดทอนคลื่นจากหุ่นลอยกันคลื่น ด้วยการทดลองในรางทดสอบคลื่นภายใต้สภาวะคลื่นปกติ โดยใช้เครื่องมือทางเลือกหรือวิธีที่ไม่ล่วงล้ำ การยืนยันความถูกต้องที่ได้จากการวัดค่าระดับผิวน้ำ ระหว่างเทคนิค การประมวลผลภาพกับวิธีมาตรวัดคลื่นแบบดั้งเดิม แสดงให้เห็นถึงผลลัพธ์ที่ดี และมีผลที่แตกต่างกัน เพียงเล็กน้อย ผลการทดลองแสดงให้เห็นว่า การลดทอนคลื่นจากหุ่นลอยกันคลื่น มีค่าสัมประสิทธิ์การส่งผ่าน ลดลงเมื่อค่าความลึกน้ำเพิ่มขึ้น ความกว้างสัมพัทธ์ของหุ่นลอย ความชันคลื่น และระยะจมน้ำสัมพัทธ์มากขึ้น นอกจากนี้ ยังพบว่าหุ่นลอยกันคลื่นแบบเดี่ยวและแบบคู่ มีค่าสัมประสิทธิ์การส่งผ่านประมาณ 0.50 ถึง 95 และ 0.40 ถึง 90 ตามลำดับ

คำสำคัญ : เชื้อกันคลื่น / แบบจำลองทางกายภาพ / วิศวกรรมชายฝั่ง / พลังงานคลื่น

* Corresponding Author : chaiyuth.chi@kmutt.ac.th

¹ ศาสตราจารย์ ศูนย์วิจัยวิศวกรรมและการจัดการน้ำ (วารี) ภาควิชาวิศวกรรมโยธา

² นักวิจัย ศูนย์วิจัยวิศวกรรมและการจัดการน้ำ (วารี) ภาควิชาวิศวกรรมโยธา

Investigation of Wave Transmission of Floating Breakwaters

Chaiyuth Chinnarasri^{1*} and Khomsan Viriyakijja²

King Mongkut's University of Technology Thonburi, Bang Mod, Thung Khru, Bangkok 10140

Abstract

The wave attenuation of floating breakwaters was investigated with experiments in a wave flume under regular wave conditions using an alternative tool or non-intrusive method. The validation of two measurements between the image processing technique and conventional wave gauge, compared with water surface elevation results, showed good agreement with a slight mismatch. The experimental results indicate that the wave attenuation of floating breakwater is characterised by a decrease in transmission coefficient with increasing water depth, and is relative to the width, wave steepness and relative draft of the floating breakwater. Additionally, it was found that single and double floating breakwaters have the transmission coefficient about 0.50 to 0.95, and 0.40 to 0.90, respectively.

Keywords : Breakwater / Physical Model / Coastal Engineering / Wave Energy

* Corresponding Author : chaiyuth.chi@kmutt.ac.th

¹ Professor, Water Resources Engineering & Management Research Center (WAREE).

² Researcher, Water Resources Engineering & Management Research Center (WAREE).

1. INTRODUCTION

Coastal areas are significant ecosystems where life and the environment coexist. Recent coastal erosion problems are one of the most hazardous phenomena, causing damage to natural resources, socio-economics, residential infrastructure and commercial activities. To reduce the erosion problem, various types of structural measures have been used to attenuate the intensity of wave energy.

The floating breakwater (FB) is an interesting structural measure that is widely used to protect areas from wave disturbances, especially in low-lying tranquil areas, as its structure can decrease wave intensity. The types of FB can be mainly divided into four groups: box; pontoon; mat and tethered float. The FB is of interest because it does not disturb seabed wildlife, facilitates flexible transportation and is suitable for small wave heights and soft seabeds [1 - 2].

The performance of a Y-frame FB, a trapezoidal pontoon assembly with a row of pipes of suitable length, was investigated by Mani [3]. The experimental results show that fixing a row of pipes of a certain length and at a certain interval at the bottom of a trapezoidal float reduces the width to wave length ratio to around 0.15, which leads to a transmission coefficient of less than 0.5 at an optimal cost. Murali and Mani [2] proposed a cost effective FB, the cage FB, which was developed by compounding two Y-frame FBs. The width of the FB to wave length ratio requirement can be reduced to 0.15 for the same structural performance [2].

Koutandos et al. [4] carried out physical experiments to explore the response of four different FB configurations under regular and irregular waves. The results showed that the single fixed was highly reflective, whereas the heave motion had lower reflection. The most efficient structural configuration was the double fixed. Considering cost efficiency, the single fixed with an attached plate was an optimal

alternative. Dong et al. [5] studied the interaction of FBs (box type) under regular waves with and without currents. These consisted of a single box, a double box and the board net, which used an anchor and string as the mooring system. The findings revealed that the board net is simple, inexpensive and effective for protecting underwater animals. Wang and Sun [6] examined a porous FB constructed from four layers of a large number of diamond shaped blocks. The proposed FB can decrease incident wave height more, by dissipating wave energy, than by reflection effects. With regards to other breakwater structures, Neelamani and Gayathri [7], for example, studied the hydrodynamic performance of a twin horizontal plate barrier on pile groups with seven different clearances between two plates. Koraim [8] investigated a horizontal half-pipe breakwater, which consists of one, two and three rows of half pipes suspended on piles. Chuenchai et al. [9] investigated wave run-up on stepped slopes in a flume and found that the wave run-up decreased as the riser heights increased, due to increasing friction.

All previously mentioned studies used conventional wave gauges to investigate experiments in a wave flume laboratory. As a new technology, image processing techniques are used widely in many studies as an alternative method.

The main concept of image processing techniques is the transformation of the time domain, represented in the image frames from the charge-coupled device (CCD) video camera, into the frequency domain, represented by digital forms of water surface elevation at points of interest [10]. In coastal and ocean laboratories, image processing from a CCD video camera is still an interesting approach to be applied in wave flume measurements.

For example, Erikson and Hanson [10] studied quantitative wave and morphodynamic data in a wave flume using video images. All three steps, image

capture, rectification and data extraction, were achieved using MATLAB.

Bonmarin et al. [11] attempted to measure steep wave characteristics in a flume. The surface wave profiles were obtained by complicated image analysis processes. Foote and Horn [12] experimentally monitored the hydrodynamics of a swash zone using video techniques applied with geographical information systems (GIS) or ArcView. The wave profile was analysed in a wave flume facility using the Mexican hat wavelet transform and GVF snake image-based techniques [13 - 14]. Umeyama and Shintani [15] applied an image processing technique, representing a video recording system, to visualise wave run-up and mixing of the upper layer (fresh water) and lower layer (salt water) on the slope in a 2D wave flume.

Eaket et al. [16] established a computer algorithm based on the collinearity condition to measure three dimensions of dynamic unsteady open channel flows, such as dam-break scenario cases. For the

calibration approach, 21 wooden blocks of known position and varying height were placed on a grid on the experimental floor to calibrate the cameras. Computer vision was used to detect the water surface in a wave flume by side wall observations. Furthermore, the system was applied to detect the motion of oil boom floating bodies [17].

The details of former studies are the motivation to propose an alternative technique for observing ocean and coastal systems in a hydraulics laboratory. The main objective of this study is to apply the image processing technique in order to investigate the performance of FBs on the wave transmission coefficient.

2. EXPERIMENTS

In this section, we briefly describe the test facilities, model details and instrumentation. The wave flume was 1.0 m wide, 27.0 m long and 1.0 m deep, as shown in Figure 1, and comprised of a rigid steel bed

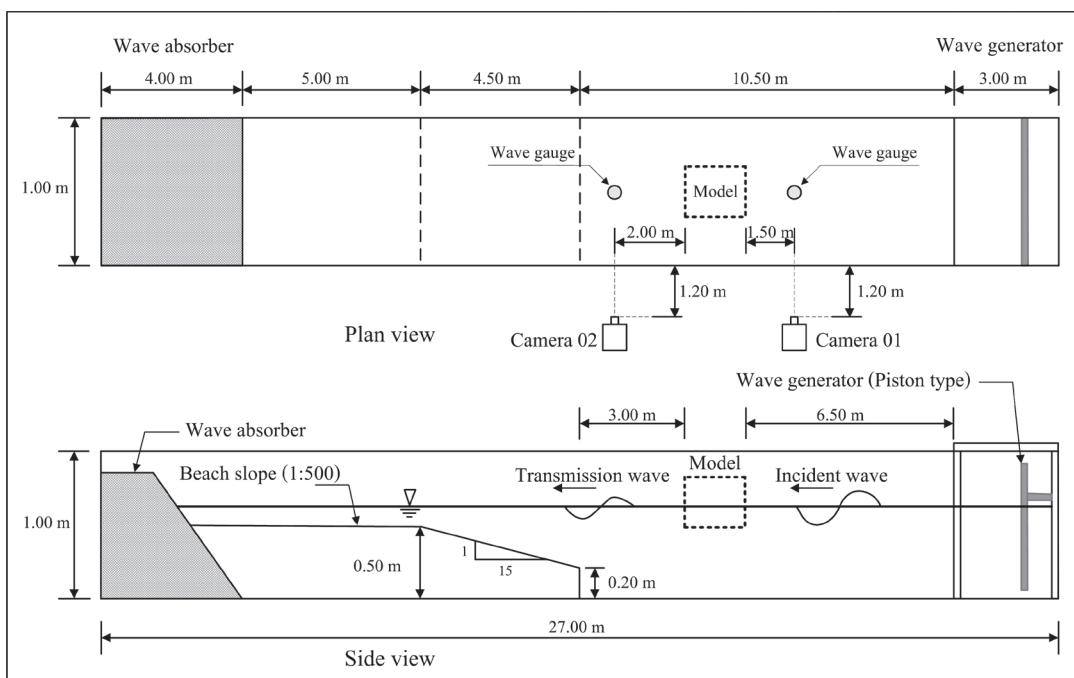


Figure 1 Experimental set-up

with side walls made of both solid steel and acrylic sheets. The end of the flume had a wave absorber made of a stone pile to reduce reflection waves. Waves were generated using a piston-type DC servo motor that can generate both regular and irregular waves. The FB position was located about 6.50 m from the wave generator. Two capacitance wave gauges (CH-403A & CHT4-40, Kennek) were placed in front of and behind the FB. The frequency of sampling data was 50Hz.

A box-shaped FB was fabricated from aluminium sheets and consisted of a rectangular box (thickness 5 mm) and side plate (thickness 3 mm). Physical 1:5 scale models of the FB were divided into two modules: single ($0.25 \times 0.50 \times 0.15$ m), as shown in Figure 2 (a), and double ($0.50 \times 0.50 \times 0.15$ m) as shown in Figure 2 (b). The model was restrained with a heavy steel plate on the flume bed by four steel cable mooring lines, each of a fixed length of about 88 cm. The clearance between the model and side wall of the

flume was 25 cm. The side plates in the models can be shifted in three draft levels of the FB. For the single and double FBs, the draft levels were 11.50, 16.50, and 21.50 cm, and 10.50, 15.50, and 20.50 cm, respectively.

Video cameras with frame rates of about 30 Hz were used as the measurement tools in the wave flume. The wave characteristics were analysed from the water surface elevation data, measured using video cameras and the image processing method. This method has good agreement with the capacitance wave gauge (sampling rate of about 50 Hz). The two wave probes, KENNEK type CH-403A and CHT4-40, were used with exact calibration in each experiment. Two video cameras were installed exactly perpendicular about 1.20 m from the acrylic side wall. The first camera was placed about 1.50 m in front of the model. As the position of the FB can move slightly due to the wave force, the second camera was placed about 2.0 m from the back of the model.

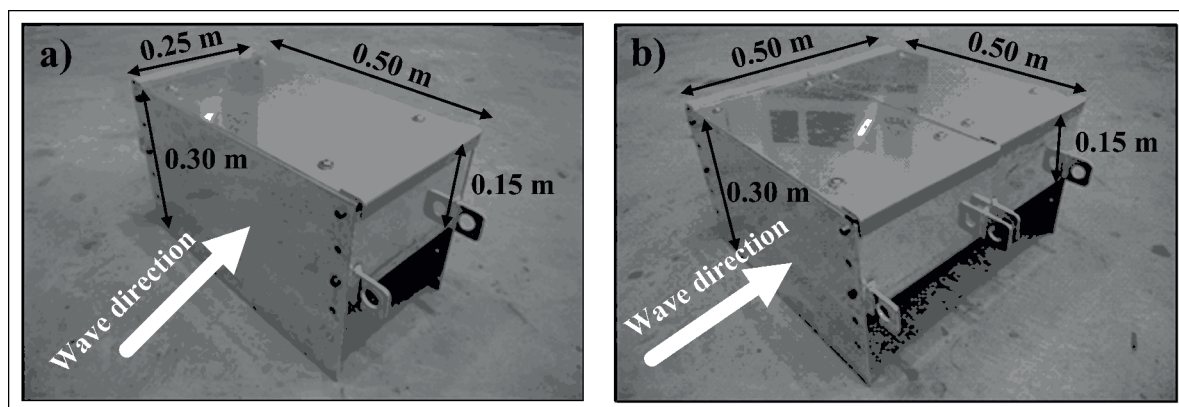


Figure 2 Physical models : a) Single floating breakwater; b) Double floating breakwater

Wave data were acquired using video cameras for a duration of 60 s at a frequency rate of 30 Hz. In the experiments, the regular wave had at least 12 wave loops, and the recording needed to finish prior to the production of the reflected waves. There were three still water depths of 60, 65 and 70 cm. The wave

height, wave length and wave period varied in the ranges of 5.65–13.84 cm, 65 – 400 cm and 0.60 – 1.60 s, respectively. 162 runs with the existence of FBs were carried out using image processing techniques described in the following sections.

3. IMAGE PROCESSING TECHNIQUES

The methodology presented in this study involved the use of a video camera as a versatile instrument in wave flume measurements. The sequence of process steps was as follows. First, the point of water surface elevation was defined and a scaling mark was placed on the side flume at the investigation point. Second, two video cameras were mounted at a suitable distance from the target plane depending on the desired data resolution. Third, the recording frame was arranged into the line of the still water level and the camera level was adjusted both vertically and horizontally. Fourth, a uniformly solid background was set behind the video cameras to block the reflection shadow from unwanted objects. Finally, the video cameras began to record the varying water surface elevations. The accuracy of this method is of utmost importance and consists of three factors: image quality, algorithm performance and exact calibration [18].

3.1 Image quality

Noise, or an unwanted or disturbed signal in the image, is the main factor that causes low image quality. There are many ways to deal with noise reduction in the experiments. For example, the CCD video camera was mounted about 1.20 m from the clear acrylic side wall of the wave flume for the appreciated image boundary. To create an obvious contrast between the water and background, the opposite side wall was made of a dark blue steel plate. A solid homogeneous board was placed behind the CCD camera to cope with any reflected shadows in the frame of the monitoring area. Furthermore, the light around the laboratory area was controlled to reduce noise by using uniform fluorescent lights hanging on top of the wave flume in all experimental runs.

3.2 Algorithm performance

Edge detection is a technique commonly used in image processing and many edge detectors are available today, such as Roberts, Sobel, Prewitt, Laplacian and Canny operators. The Canny edge detector, invented by John Canny in 1986, was used in MATLAB for wave observation since it is an optimal, powerful and effective edge detector [19 - 22]. The basic steps are divided into four parts as follows. First, smoothing was performed using a Gaussian filter, which filters out noise from the image, and the potential edges were then selected as a candidate pixel image. Second, gradient analysis was used to calculate the magnitude and direction of the gradient using a first-order derivative method for edge strength. Third, non-maximum suppression was used to thin the edge, leaving only the pixel at the top of each edge. Finally, hysteresis thresholding was used to identify the edge pixel position and connect the edge boundary.

3.3 Exact calibration

As previously mentioned, video cameras were the base apparatus for the laboratory measurements. Most camera devices suffer from lens distortion or optical error that causes straight lines in the real world to become curved lines in the image [10, 12]. In this investigation, three approaches were used to confirm exact calibration : using an array of exact grids made of clear acrylic sheets to check the lens distortion in each camera position; mounting the camera to record data in line with the still water level in the wave flume and controlling the tilt angle of the camera to be vertically and horizontally level; and designing the algorithms to process only the middle area of the image since lens distortion barely occurs in the middle of an image.

3.4 Edge detection algorithms

A wave is a water surface elevation that continuously changes over time [23 - 24]. Therefore, the concept of designing algorithms to measure waves refers to transfer of the time domain, represented by many video image frames, to the frequency domain, represented by water surface elevation. The edge detection algorithm is a semi-automatic process that operates simply in MATLAB with exact outputs. This algorithm was used

to detect the water surface as an edge in each frame and to convert the pixels between the edge and reference point into water surface elevation. The results of the edge detection algorithm are shown in Figure 3. In this study, MATLAB was used to design such algorithms. The details of the algorithms in each step are divided into three processes as described in the following sections.

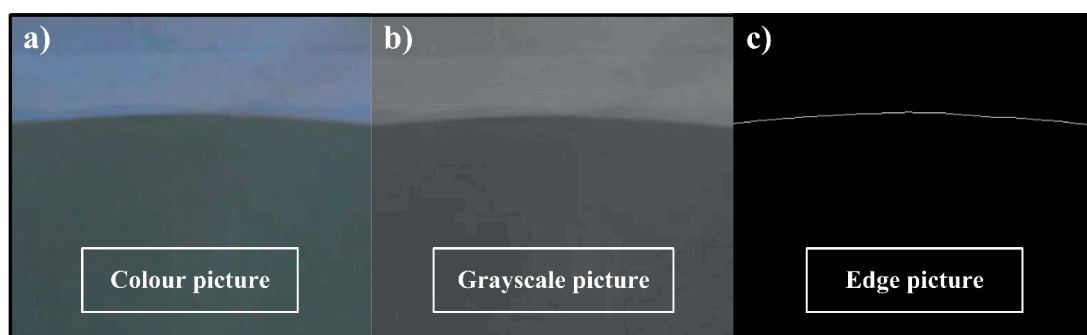


Figure 3 Results of edge detection algorithms :
a) Colour of raw picture; b) grayscale picture; c) edge picture

3.5 Preprocessing

The video of the water surface elevation at a point of interest was first extracted to sequence the image frames. Second, all frames were defined in a specific area at the centre of each frame to decrease the analysed time. In addition, this step partly reduced lens distortion since distortion occurs less frequently in the middle of frames compared with the border area. Third, the image frames were converted from RGB (three channels) to grayscale (one channel) images for effective processing.

3.6 Processing

The grayscale images were analysed using a Canny edge detector in MATLAB. At the appropriate threshold, a good binary image was obtained. The binary image was composed of two parts: i) the foreground or edge represented by the colour white

(pixel value = 1), and ii) the background represented by the colour black (pixel value = 0). The binary image was then processed using the algorithms by detecting the edge or water surface elevation, and the result was shown by referencing to the exact scale of the image. One frame was one point of water surface elevation; therefore, the sequence of image frames was equal to the continuously changing water surface elevation over time.

3.7 Post-processing

The final result from the edge detection algorithm was the relationship of the water surface elevation and monitoring position. The main wave characteristics, represented by wave height, wave period and wave length, were then acquired using zero up-crossing analysis and Hunt's empirical equation [25].

4. ANALYSIS OF WAVE TRANSMISSION

In this study, the basic assumptions and conditions are as follow: i) the characteristics of the bed material and bed slope do not change along the flume's length; ii) the density and depth of the fresh water are constant; iii) the still water level is constant in each experiment; iv) wave propagation is considered in two dimensions perpendicular to the structure; v) regular wave generation is used throughout the structure and vi) the influence of wave reflection is ignored.

4.1 Dimensional analysis

Many parameters play important roles in the

performance of an FB, as shown in Figure 4. They can be divided into two main groups. The first comprises the parameters of the waves: H_i (incident wave height); H_t (transmitted wave height); L (wave length); d (still water depth) and the second parameters of the FB: B (width of the FB) and D (draft of the FB).

The parameter ranges are listed in Table 1. All parameters are given in only the dimension of length. The transmission coefficient (C_t) can be calculated from the ratio of H_t and H_i and can be expressed in dimensionless form :

$$C_t = \frac{H_t}{H_i} = f\left(\frac{d}{L}, \frac{B}{L}, \frac{H_i}{L}, \frac{D}{d}\right) \tag{1}$$

Table 1 Ranges of parameters used in this study

Parameter	Ranges (cm)
Water depth (d)	60, 65, and 70
Wave length (L)	65 - 400
Width of FB (B)	25 for single FB 50 for double FB
Incident wave height (H_i)	5.65 - 13.84
Draft of FB (D)	11.50, 16.50, and 21.50 for single FB 10.50, 15.50, and 20.50 for double FB

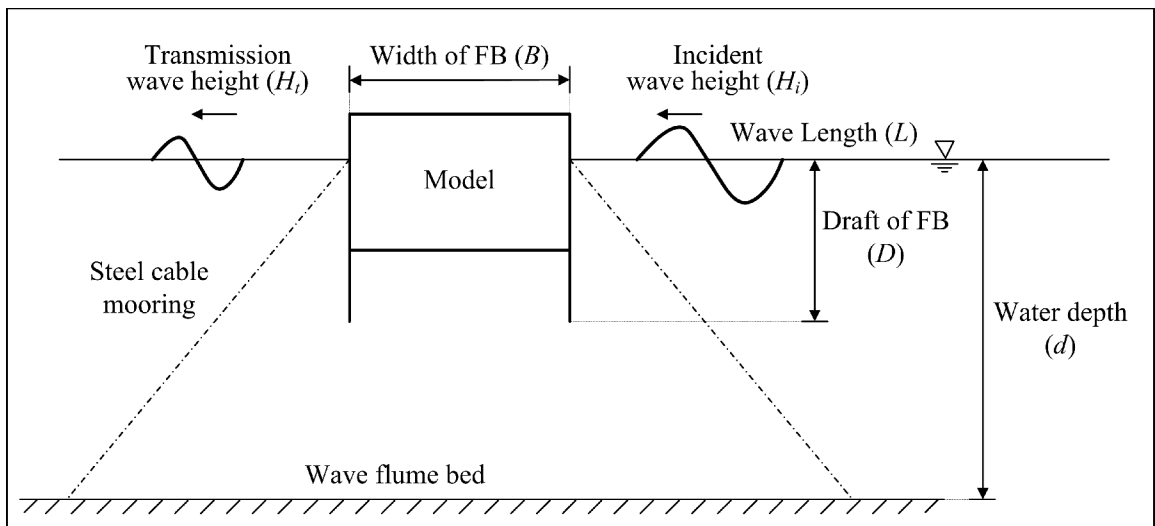


Figure 4 Parameters involved in the wave transmission

4.2 Zero up-crossing analysis

Videos of water surface elevation were obtained using CCD video cameras to analyse edge detection algorithms in MATLAB. The MATLAB results show continuous water surface elevations at the time intervals of interest. This output was used to ascertain the wave characteristics by short-term analysis and an empirical equation.

For short-term wave analysis, the relation of water surface elevation to time can be resolved using the zero up-crossing technique to obtain wave height and wave period [24, 26]. First, the reference point that passes from a negative to positive position of water surface elevation and intercepts with the reference line is defined. Second, the wave height of the first loop is the maximum difference of water surface elevation between two points on the reference line. Third, the wave period of the first loop is the time interval from the first point to the second on the reference line. Finally, these three steps along the reference line were carried out to obtain the wave height and wave period of all wave loops.

4.3 Wave energy balance

Wave propagation is carried with wave energy. Where there is a barrier, the FB cannot dissipate all of the incident wave energy. The incident wave is partially transmitted, partially reflected and partially dissipated. Theoretically, the energy equilibrium of the total wave energy can be expressed according to Eqs. (2) and (3) below [4, 8] :

$$E_i = E_t + E_r + E_l \quad (2)$$

or rewritten as

$$\frac{\rho g H_i^2}{8} = \frac{\rho g H_t^2}{8} + \frac{\rho g H_r^2}{8} + \frac{\rho g H_l^2}{8} \quad (3)$$

where E_i represents the incident wave energy, E_t is the transmission wave energy, E_r is the reflection wave

energy, E_l is the dissipation wave energy, H_i is the incident wave height, H_t is the transmission wave height, H_r is the reflected wave height and H_l is the dissipation wave height.

The reflected wave can be ignored since all of the experimental studies were finished before any reflected wave effects began. The incident and transmission waves were obtained using image processing techniques in the laboratory. Hence, the dissipation wave can be estimated as :

$$C_l = \sqrt{1 - C_t^2} \quad (4)$$

where C_l is the energy dissipation coefficient and C_t is the transmission coefficient.

4.4 Wave celerity

The wave celerity and wave length can be expressed as an empirical equation. Hunt [25] proposed the direct and accurate approximating equation :

$$\frac{C^2}{gd} = \left[y_0 + (1 + 0.6522y_0 + 0.4622y_0^2 + 0.0864y_0^4 + 0.0675y_0^5)^{-1} \right] \quad (5)$$

where $y_0 = \frac{2\pi d}{L_0}$, $L_0 = \frac{gT^2}{2\pi}$, $L = CT$,

C is the wave celerity, L is the wave length, L_0 is the wave length in the deep water zone, T is the wave period and g is the acceleration of gravity. This calculation is based on a higher order expansion method that yields a high accuracy result of about 0.1% [24].

5. RESULTS AND DISCUSSION

The image processing technique is validated to confirm its performance as an alternative tool in wave flume measurements. The performance of the FBs is then presented to investigate the effects of major parameters on the wave transmission coefficient.

5.1 Wave transmission coefficients of the FB

After development and validation of the image processing technique based on edge detection algorithms, these results were used to study the performance of the FB by comparing the wave transmission trend of both single and double module types under regular wave interactions. 162 experiments were carried out in a wide wave flume. The influential parameters of the wave properties and physical FB were considered in order to understand the change in wave mechanism.

5.2 Effect of relative water depth

The ideal FB is mostly utilised under suitable conditions in the intermediate to deep zone. The physical meaning of a relative water depth value refers

to the water wave zone. In the experiments, the C_t values of the wave decreased with relative water depth (d/L), which increased relative to the draft of the FB ($D/d = 0.1643, 0.2357, 0.3071$ for the single FB and $D/d = 0.1500, 0.2214, 0.2928$ for the double FB).

When considering the relationship in Figure 5, the relative water depths were classified into two phases. The first range is 0.20 to 0.50, or the transitional water wave zone, in which C_t decreased from 0.95 to 0.70 and 0.95–0.60 for the single and double FBs, respectively. The second range is 0.50 to 1.00, or the deep water wave zone, where C_t improved from 0.70–0.50 and 0.60–0.20 for the single and double FBs, respectively.

The shallow water waves, small values of d/L , occur by two conditions, i.e. long wave length or small water depth. Normally, for shallow water waves, the transmitted waves will reduce more due to bed friction.

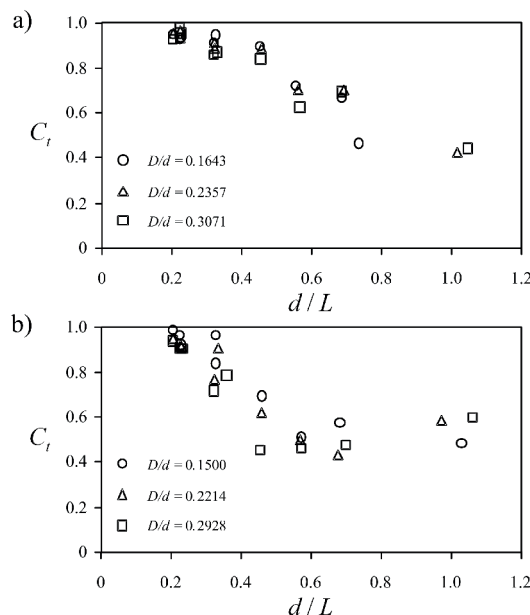


Figure 5 Effect of relative water depth on transmission coefficient : a) Single floating breakwater; b) Double floating breakwater.

In this experiment, the wave length is long enough to allow occurrence of deep water wave zone, $d/L > 0.50$. In this zone, the FB is efficient due to the sudden

change in water particle movement. This result occurred because higher d/L values or closeness to the deep water wave zone lead to maximum wave energy closer

to the water surface elevation. The turbulence caused due to this sudden change cause energy dissipation [8].

This can be explained by considering that the tension of the steel cable increases with water depth or d/L . As a result, the steel cable moorings were kept at a constant length in each case. A higher tension mooring system can block more wave energy, especially in a longer wave period. Therefore, the deep zones have a lower C_t than the shallow zones for the above reasons.

5.3 Effect of wave steepness

The strength of the wave interaction with the FB is affected by the wave steepness. Normally, the wave becomes unstable and breaks when the wave steepness value is greater than or equal to about 0.14. The effect of wave steepness (H_i/L) is clearly significant with respect to C_t in the different relative drafts of the FB (D/d). It can be seen that C_t decreases as H_i/L

increases or that flat waves (low H_i/L values) have higher C_t values than steeper waves (high H_i/L values) for all cases.

Changing H_i/L from 0.02 to 0.12 leads to a decrease in the C_t ranging from 0.95 to 0.60 and 0.90 to 0.45 for single and double FBs, respectively, as shown in Figure 6. The incident wave mechanism can dissipate with higher wave steepness. The steeper waves or shorter period waves made intense attacks on the FB, causing more turbulence in the water wave particles in front of the FB, while the flat waves or longer period waves mostly flowed through under the FB.

Scattered data were obtained from the steeper wave more than in the flat wave, especially within the H_i/L range of 0.05–0.07. This is due to the fact that the water particles are turbulently moved in the steep wave more than in the flat wave. In addition, waves developed from the transitional water wave to the deep water zone in the H_i/L range between 0.05 and 0.07.

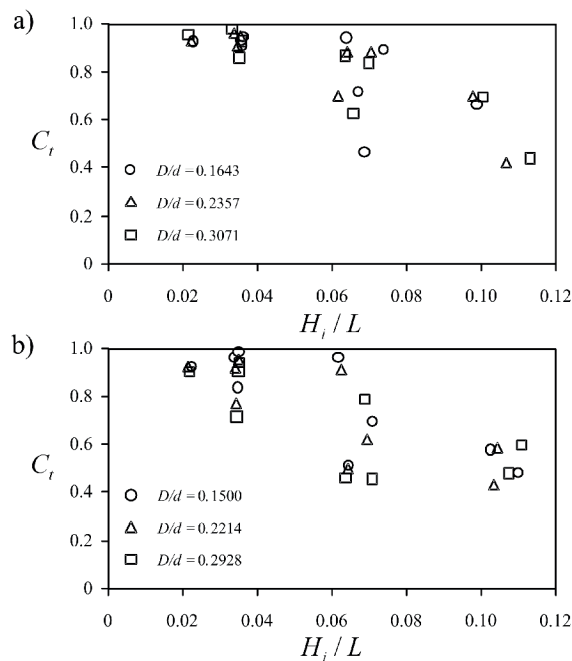


Figure 6 Effect of wave steepness on transmission coefficient : a) Single floating breakwater; b) Double floating breakwater.

The fixed breakwater mostly shows good performance in the reflection effect; however, these experiment disregards the reflective behaviour. Hence, the heave motion of the FB plays an important role in wave interaction. Due to the heave motion, short period waves flow through the structure with higher vortex intensity than long period waves. This can be explained by considering that the FB moves vertically in the difference phase with shorter waveforms, while the longer wave and structure move in the same phase. The out-of-phase waves mainly cause strong vortex motion and energy dissipation [4].

5.4 Effect of wave celerity

The wave celerity can be calculated using Eq. (5). The reduction of wave celerity was considered for both single and double FBs under several regular wave conditions. The FB was linked to the flume bed by two steel cables on each side. Therefore, the two steel cables in front of the FB were tightened by wave attack, and the opposite cable supported the balance of the structure. Under wave interactions, the FB can move in the vertical and lateral directions.

The single module cannot obviously decrease wave celerity while the double module showed good performance of around 20–40%, especially for the wave steepness intervals greater than 0.09. In the single module cases, the low-level turbulence flow occurred compared with the double module. Additionally, the steeper waves can be broken to dissipate more wave energy and reduce the wave celerity with greater disturbance.

5.5 Effect of relative width and draft

The relative width (B/L) can refer to the rigidity of the breakwater and size of the disturbance. The transmission coefficient of the wave shows an inversely proportional trend with B/L at the same trend of relative water depth (d/L). For single FBs ($B = 25$ cm), the C_t decreases from 0.95 to 0.40 as B/L increases from 0.10 to 0.40, as shown in Figure 7(a). When the width of the FB increases from 25 to 50 cm or double FB, the wave transmission decreases. This change can improve the efficiency by about 10% as shown in Figure 7(b).

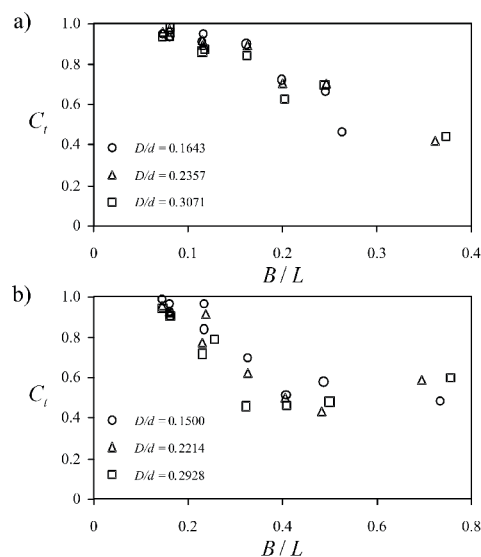


Figure 7 Effect of relative width on the transmission coefficient : a) Single floating breakwater; b) Double floating breakwater.

The explanation for this observation is that the concentrated wave energy stays mainly near the water surface elevation, thus higher B/L values approach the large rigidity in blocking wave energy, and the region of shear friction on the breakwater body. As such, the width of the FB plays a significant role in the efficiency of wave transmission reduction. Hence, the effective width can be utilised depending on the wave conditions and cost.

Enhanced FB performance was studied by adding an obstacle or smooth plate to two sides of the structure. The effect of the different relative drafts of the single and double FBs (D/d) on C_t when increasing D/d by increasing the distance of the submerged FB in three steps (5 cm/step), which leads to a slight decrease of about 5% in C_t for the double FB. In contrast, the single FB has the same trend but the effect is not as clear. The FB draft shows good performance with respect to

complete reflection. Due to the conditions investigated here, the effect of relative draft cannot occur obviously. However, it can be implied that the factor of relative draft has less influence than FB width in technical terms but not for cost effectiveness.

The effect of the number of the FBs is given in Figure 8 with $n = 1$ for a single FB and $n = 2$ for a double FB. The double FB can reduce the transmission coefficient more significantly than the single FB by about 10% although there are similar phenomena. The performance of this structure showed maximum ranges of about 40–60% for the deep zones ($0.5 < d/L < 1.0$) and steeper waves ($0.06 < H_i/L < 0.12$). The shear friction on the surface of the structure and changing hydrodynamics of the wave are an important mechanism in dissipating wave energy. In addition, the number of FBs can multiply disturbance and block wave motion.

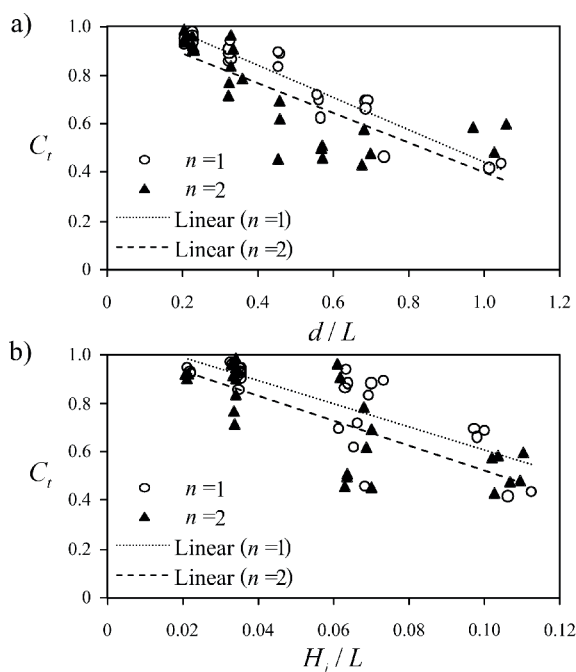


Figure 8 Effect of number of floating breakwater on the transmission coefficient : a) varied relative depth; b) varied wave steepness

The C_t values of the FBs in the experimental study were used with regression analysis. The general form selected in this work was the linear form in Eq. (6) below. The equation can be rewritten in dimensionless parameters as in Eq. (7).

$$Y = \beta_0 + \beta_1 x_1 + \beta_2 x_2 + \beta_3 x_3 + \dots + \beta_n x_n \quad (6)$$

$$C_t = \beta_0 + \beta_1 \left(\frac{d}{L}\right) + \beta_2 \left(\frac{B}{L}\right) + \beta_3 \left(\frac{H_i}{L}\right) + \beta_4 \left(\frac{D}{d}\right) \quad (7)$$

A comparison between the observed and predicted transmission coefficients shows good agreement. The coefficient of determination for linear analysis is 0.720 ($R^2 = 0.720$). Statistical Pearson correlation results

show that the primary parameters affecting C_t are relative depth, relative width of the FB and wave steepness, whereas, relative draft is a secondary parameter with less of a relationship with C_t . The standardised coefficient represents the most influential parameter on C_t , indicating that all of the parameters follow an opposite trend.

With the ranges of parameters used in this study (Table 1), the multiple linear regression based on Eq. (7) was analysed to obtain the unstandardised coefficients (Beta) in Table 2. The ranges of dimensionless forms of parameters are also listed in Table 2.

Table 2 Statistical details of the linear regression analysis and ranges of dimensionless ratio

Parameters	Ranges of dimensionless ratio	Pearson correlation	Standardised coefficient	Unstandardised coefficient (Beta)
C_t	-	1.00	-	1.00
d/L	0.20 - 1.00	-0.798	-0.211	-0.162
B/L	0.10 - 0.80	-0.793	-0.426	-0.469
H_i/L	0.02 - 0.10	-0.777	-0.267	-1.653
D/d	0.15 - 0.35	-0.070	-0.095	-0.255
Constant	-	-	-	1.116

The suggested FB equation can be firstly introduced and expressed as :

$$C_t = 1.116 - 0.162 \left(\frac{d}{L}\right) - 0.469 \left(\frac{B}{L}\right) - 1.653 \left(\frac{H_i}{L}\right) - 0.255 \left(\frac{D}{d}\right) \quad (8)$$

6. CONCLUSIONS

This paper presents wave attenuation of FBs using a non-intrusive observation system based on image processing techniques in a wave flume experiment. All wave data were obtained from CCD video cameras

in the side-view position of the wave flume. The edge detection algorithm of this image processing method is an effective semi-automatic alternative for water surface elevation observation systems in wave flumes. The validation of this approach between the CCD

video camera and traditional wave gauge has good agreement in terms of water surface elevation at 0.97 of the determination coefficient.

The transmission coefficient decreases as the main factors, such as relative water depth, relative width of the FB and wave steepness, increase. Relative draft is a secondary factor with significant influence on the FB. Moreover, it was found that a single FB has a transmission coefficient of about 0.50 to 0.95. A double FB can improve efficiency and has a transmission coefficient of about 0.40 to 90.

A simple empirical equation used to estimate the wave transmission coefficient through the FB was formulated by linear regression analysis. The results of the equations show good agreement between the experimental and theoretical results represented by a determination coefficient of about 0.72.

7. ACKNOWLEDGEMENTS

The authors would like to thank the National Research University Project (NRU) of Thailand's Office of the Higher Education Commission and Department of Civil Engineering KMUTT (Contract number CE-KMUTT-FTERO 5702) for financial support for this study. We are also grateful to Dr. Thamnoon Rasmeemasuang, Dr. Anurak Sriaiyawat and Dr. Supanee Tanathong for their valuable recommendations and suggestions.

8. REFERENCES

1. McCartney, B.L., 1985, "Floating Breakwater Design," *Journal of Waterway, Port, Coastal, and Ocean Engineering*, 111 (2), pp. 304-318.
2. Murali, K. and Mani, J.S., 1997, "Performance of Cage Floating Breakwater," *Journal of Waterway, Port, Coastal, and Ocean Engineering*, 123 (4), pp. 172-179.
3. Mani, J.S., 1991, "Design of Y-frame Floating Breakwater," *Journal of Waterway, Port, Coastal, and Ocean Engineering*, 117 (2), pp. 105-119.
4. Koutandos, E., Prinos, P. and Gironella, X., 2005, "Floating Breakwater under Regular and Irregular Wave Forcing : Reflection and Transmission Characteristics," *Journal of Hydraulic Research*, 43 (2), pp. 174-188.
5. Dong, G.H., Zheng, Y.N., Li, Y.C., Teng, B., Guan, C.T. and Lin D.F., 2008, "Experiments on Wave Transmission Coefficients of Floating Breakwaters," *Ocean Engineering*, 35 (8-9), pp. 931-938.
6. Wang, H.Y. and Sun, Z.C., 2010, "Experimental Study of a Porous Floating Breakwater," *Ocean Engineering*, 37 (5-6), pp. 520-527.
7. Neelamani, S. and Gayathri, T., 2006, "Wave Interaction with Twin Plate Wave Barrier," *Ocean Engineering*, 33, pp. 495-516.
8. Koraim, A.S., 2013, "Hydrodynamic Efficiency of Suspended Horizontal Rows of Half Pipes used as a New Type Breakwater," *Ocean Engineering*, 64, pp. 1-22.
9. Chuenchai, W., Pholyeam, N., Phetchawang, S. and Rasmeemasuang, T., 2013, "Wave Run-up on Stepped Slopes," *KMUTT Research and Development Journal*, 36 (3), pp. 329-340. (In Thai)
10. Erikson, Li H. and Hanson, H., 2005, "A Method to Extract Wave Tank Data using Video Imagery and its Comparison to Conventional Data Collection Techniques," *Computers and Geosciences*, 31 (3), pp. 371-384.
11. Bonmarin, P., Rochefort, R. and Bourguel, M., 1989, "Surface Wave Profile Measurement by Image Analysis," *Experiments in Fluids*, 7, pp. 17-24.
12. Foote, M. and Horn, D., 1999, "Video Measurement of Swash Zone Hydrodynamics," *Geomorphology*, 29 (1-2), pp. 59-76.

13. Lee, H.S. and Kwon, S.H., 2003, "Wave Profile Measurement by Wavelet Transform," *Ocean Engineering*, 30 (18), pp. 2313-2328.
14. Yao, A. and Wu, C.H., 2005, "An Automated Image-based Technique for Tracking Sequential Surface Wave Profiles," *Ocean Engineering*, 32 (2), pp. 157-173.
15. Umeyama, M. and Shintani, T., 2004, "Visualization Analysis of Run-up and Mixing of Internal Waves on an Upper Slope," *Journal of Waterway, Port, Coastal, and Ocean Engineering*, 130 (2), pp. 89-97.
16. Eaket, J., Hicks, F. and Peterson, A., 2005, "Use of Stereoscopy for Dam Break Flow Measurement," *Journal of Hydraulic Engineering*, 131 (1), pp. 24-29.
17. Iglesias, G., Ibáñez, O., Castro, A., Rabuñal, J.R. and Dorado, J., 2009, "Computer Vision Applied to Wave Flume Measurements," *Ocean Engineering*, 36 (14), pp. 1073-1079.
18. Wang, C.C., Chen, P.C. and Liao, C.Y., 2012, "Application of CCD Cameras as a Versatile Measurement Tool for Flume Tank," *Ocean Engineering*, 42, pp. 71-82.
19. Gonzalez, R.C. and Woods, R.E., 2002, *Digital Image Processing*, Prentice-Hall, New Jersey, 793 p.
20. Jain, R., Kasturi, R. and Schunck, B.G., 1995, *Machine Vision*, McGraw-Hill, New York, 549 p.
21. Marques, O., 2011, *Practical Image and Video Processing Using MATLAB*, Wiley/IEEE Press, New Jersey, 639 p.
22. McAndrew, A., 2004, *Introduction to Digital Image Processing with MATLAB*, Thomson, Singapore, 509 p.
23. Hughes, S.A., 1993, "Physical Models and Laboratory Techniques in Coastal Engineering," in *Advanced Series on Ocean Engineering*, Vol. 7, World Scientific, Singapore, 568 p.
24. Kamphuis, J.W., 2000, "Introduction to Coastal Engineering and Management," in *Advanced Series on Ocean Engineering*, Vol. 16, World Scientific, Singapore, 437 p.
25. Hunt, J.N., 1979, "Direct Solution of Wave Dispersion Equation," *Journal of Waterways, Port, Coastal, and Ocean Division*, ASCE 105 (4), pp. 457-459.
26. Holthuijsen, L.H., 2007, *Wave in Oceanic and Coastal Waters*, Cambridge University Press, New York, 387 p.